Environmental Science & Technology

Article

Cite This: Environ. Sci. Technol. 2018, 52, 2538−2548

pubs.acs.org/est

# Unifying Concepts Linking Dissolved Organic Matter Composition to Persistence in Aquatic Ecosystems

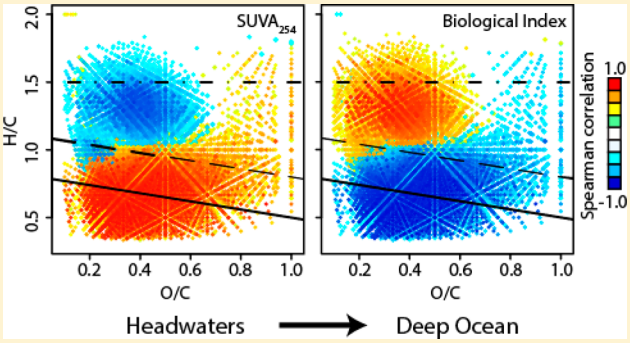
Anne M. Kellerman,*[,†] François Guillemette,[†,∥] David C. Podgorski,[†,‡] George R. Aiken,[§] Kenna D. Butler,[§] and Robert G. M. Spencer[†]

[†]National High Magnetic Field Laboratory Geochemistry Group and Department of Earth, Ocean, and Atmospheric Science, Florida State University, Tallahassee, Florida 32306, United States

[§]U.S. Geological Survey, 3215 Marine Street, Boulder, Colorado 80303, United States

Supporting Information

**ABSTRACT:** The link between composition and reactivity of dissolved organic matter (DOM) is central to understanding the role aquatic systems play in the global carbon cycle; yet, unifying concepts driving molecular composition have yet to be established. We characterized 37 DOM isolates from diverse aquatic ecosystems, including their stable and radiocarbon isotopes ($\delta^{13}$C-dissolved organic carbon (DOC) and $\Delta^{14}$C-DOC), optical properties (absorbance and fluorescence), and molecular composition (ultrahigh resolution mass spectrometry). Isolates encompassed end-members of allochthonous and autochthonous DOM from sites across the United States, the Pacific Ocean, and Antarctic lakes. Modern $\Delta^{14}$C-DOC and optical properties reflecting increased aromaticity, such as carbon specific UV absorbance at 254 nm ($SUVA_{254}$), were directly related to polyphenolic and polycyclic aromatic compounds, whereas enriched $\delta^{13}$C-DOC and optical properties reflecting autochthonous end-members were positively correlated to more aliphatic compounds. Furthermore, the two sets of autochthonous end-members (Pacific Ocean and Antarctic lakes) exhibited distinct molecular composition due to differences in extent of degradation. Across all sites and end-members studied, we find a consistent shift in composition with aging, highlighting the persistence of certain biomolecules concurrent with degradation time.




## INTRODUCTION

Dissolved organic matter (DOM) is a diverse mixture of compounds forming gradients of composition and biogeochemical reactivity derived from allochthonous, autochthonous, and microbial sources. Dominant controls on DOM composition, and thus reactivity and persistence, may be intrinsic (e.g., elemental composition or structure) or extrinsic (e.g., environmental controls) factors. This remains a topic of debate across ecosystems, from soils[1,2] to freshwaters[3] and the oceans.[4−6] The decrease in the reactivity of DOM from headwaters to the ocean can largely be explained by residence time.[7] However, the molecular underpinnings of this relationship and whether reactivity is controlled by intrinsic or extrinsic factors remains unresolved, as to date no study has examined compositional changes across the aquatic continuum.

In freshwaters, DOM reactivity (e.g., metal binding, biological, and photochemical degradation) has been linked to chemical composition.[8−10] Thus, detailed chemical characterization of DOM examining composition, source, and reactivity has become increasingly common.[9−11] Optical measurements (e.g., absorbance and fluorescence) have been extensively used for characterizing DOM due to rapid sample throughput, low analytical cost, and ability to trace DOM composition. Past regional studies have linked optical DOM measurements to composition (e.g., temperate and boreal ecosystems),[3,12−15] whereas others have related optical characteristics to sources.[16−18] The operationally defined humic and fulvic acids have long been credited as a major source of red-shifted fluorescence from allochthonous sources and blue-shifted fluorescence from autochthonous sources.[18] "Protein-like" fluorescence has often been attributed to microbial sources[19,20] and related to amino acid concentrations in the ocean,[21] but also linked to lignin phenols and tannins.[22,23] Regional studies have highlighted relationships between optical properties measured on whole water DOM, and Fourier transform ion cyclotron resonance mass spectrometry (FT-ICR MS) detected DOM molecules in temperate,[13] boreal[3,12] and subtropical systems[24] in solid-phase extracted DOM. In marine systems, compounds most highly associated with $\Delta^{14}$C-depleted DOC in the ocean (i.e., the most persistent compounds) have been associated with a narrow range of molecular composition (H/C: 1.17 ± 0.13; O/C: 0.52 ± 0.10; molecular mass: 360 ± 28 and 497 ± 51 Da), termed the "island of stability" (IOS).[4] The persistence of molecules smaller than 1 kDa supports the

Received: October 30, 2017
Revised: February 1, 2018
Accepted: February 2, 2018
Published: February 2, 2018

ACS Publications © 2018 American Chemical Society



DOI: 10.1021/acs.est.7b05513
Environ. Sci. Technol. 2018, 52, 2538−2548

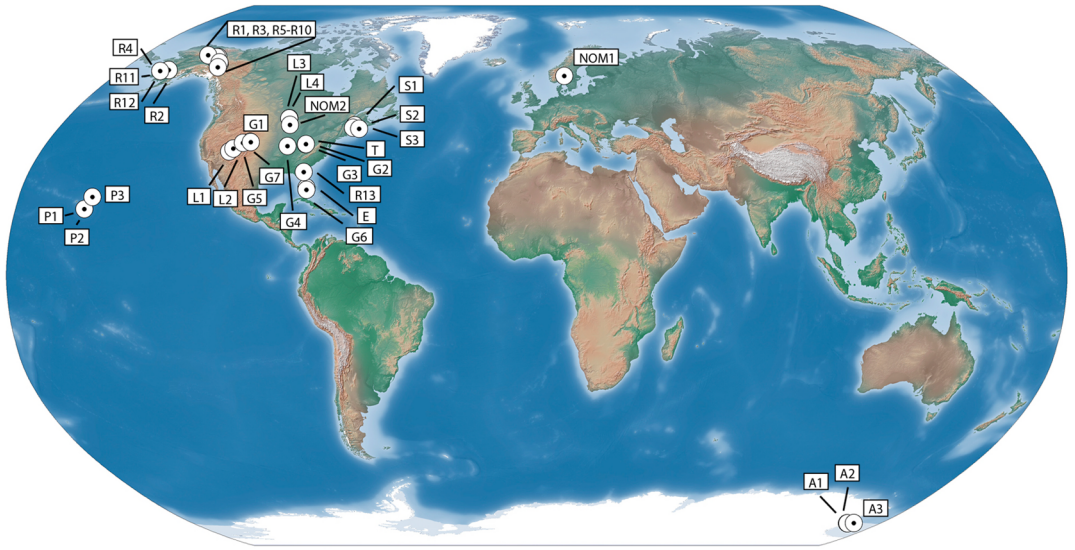



**Figure 1.** Map of the sampling locations. The white circles indicate the sampling locations of the current study ($n$ = 37). Table 1 and SI Table 1 contain coordinates and compositional data. Made with Natural Earth.

size-reactivity continuum proposed in the ocean, which suggests apparent size controls reactivity.[25] Studies conducted in boreal lakes have shown similar directional shifts in DOM composition with increasing water residence time,[3,26] however, the link between persistence and composition has never been assessed across the full continuum of aquatic ecosystems.

In this study, we examine the optical properties, stable and radiocarbon isotopes, and FT-ICR MS derived molecular composition, all measured on isolated DOM, from a diverse suite of 37 aquatic ecosystems (Supporting Information (SI) Table 1). These isolates have been established as highly diverse end-members of DOM sources and composition[27] and were chosen to evaluate if patterns in DOM sources, optical properties, and molecular composition generated in past regional studies[3,12,13,24] hold across a global gradient of aquatic systems. These isolates were further chosen to reduce artifacts of comparing solid-phase extracted DOM, necessary for FT-ICR MS analysis, to whole water optical and isotopic measurements. We hypothesize that the persistence of DOM will be inherently linked to its composition across all aquatic environments and that the most aged DOM pools will be characterized by a less diverse array of compounds, dominated by microbial degradation products.

## MATERIALS AND METHODS

**DOM Isolation.** Hydrophobic organic acids (HPOA; $n$ = 22), fulvic acids (FA; $n$ = 13), and natural organic matter (NOM; $n$ = 2) were isolated from a wide variety of aquatic systems, predominantly freshwater systems across the United States, but also in the Pacific Ocean, Antarctica, and a reservoir in Norway (Figure 1, SI Table 1). Samples were taken from surface waters unless otherwise noted in Table 1. HPOAs and FAs were isolated using standard methods. Briefly, DOM was passed through XAD-8 resin, eluted with aqueous NaOH, immediately acidified to pH 2 with concentrated HCl, rinsed with deionized water, hydrogen-saturated using ion exchange, and then lyophilized.[28−30] FA fractions differ from HPOA in that FA is the remaining fraction of HPOA after the humic acid portion has been removed (i.e., insoluble at pH 2). FA generally composed >95% of the HPOA and removing the humic acid fraction was eventually discontinued over the years.[28] Four isolates (Suwannee River FA (R13), Nordic Reservoir NOM (NOM1), Upper Mississippi NOM (NOM2), and Pony Lake FA (A3)) were obtained from The International Humic Substances Society, two of which were NOM samples isolated using reverse osmosis/electrodialysis.[31] All FA samples included in the study, with the exception of the two FAs obtained from the International Humic Substances Society, were isolated before 1990; thereafter, samples were isolated as HPOA.

**Absorbance and Fluorescence Spectroscopy.** Isolates were redissolved in Milli-Q to a final concentration of 10 mg C $L^{-1}$ to measure carbon-normalized absorbance and fluorescence properties. Absorbance and excitation−emission matrices (EEMs) were collected using a Horiba Scientific Aqualog. Scans were collected over 5 nm increments with excitation wavelengths from 230 to 800 nm and emission wavelengths from 250 to 800 nm. Samples were run with 1 s integration time. Upon detector saturation, samples were rerun using 0.5 s integration time ($n$ = 5). Two of the Pacific Ocean samples had low fluorescence and were rerun using an integration time of 10 s (NELHA, Pacific Ocean, 21 m (P1), and Pacific Ocean, 240 m (P3), see Table 1 and SI Table 1).

Carbon specific UV-absorbance at 254 nm ($SUVA_{254}$),[14] spectral indices, such as biological index (BIX),[32] fluorescence index (FI),[27] and humification index (HIX),[33,34] and parallel factor (PARAFAC) analysis were used to analyze the optical data. $SUVA_{254}$ and HIX reflect aromaticity and higher values often indicate terrestrial sources.[14,18,33,34] Conversely, high BIX and FI are often related to higher fractions of microbially produced DOM.[18] PARAFAC analysis was conducted using the drEEM toolbox[35] in Matlab and decomposed the signal of five fluorescence components (SI Figure 1), all of which have been previously identified. This was confirmed by comparing the components to the OpenFluor database.[36] The 5-component model explained 99.85% of the variance, and while there was evidence of a residual fluorescence peak at Ex/Em = 270/300 in some of the samples, we did not consider a 6-component model based on visual inspection of the sixth component. The five-component model had a low core consistency (1.3%), but the model was validated using split-half analysis with four splits (SI Figures 1 and 2, SI Table 2). The percent contribution of each component


DOI: 10.1021/acs.est.7b05513
Environ. Sci. Technol. 2018, 52, 2538−2548

**Table 1. Site-Specific Source, Age, and Compositional Data**[a]

| NMDS label | site | $SUVA_{254}$ (L mg $C^{-1}$ $m^{-1}$) | $A_{250}/A_{365}$ | $S_{275-295}$ ($nm^{-1}$) | $S_R$ | $Fmax_{total}$ | % component 1 | % component 2 | % component 3 | % component 4 | % component 5 | fluorescence index (FI) | humification index (HIX) | biological index (BIX) | assigned formulas (#) | condensed aromatics (% RA) | polyphenolic (% RA) | unsaturated and phenolic (%RA) | aliphatic (%RA) | island of stability (IOS; % RA) | $\partial^{13}C$-DOC, ‰ | $\Delta^{14}C$-DOC, ‰ |
|---|---|---|---|---|---|---|---|---|---|---|---|---|---|---|---|---|---|---|---|---|---|---|
| R1 | Upper Birch R. | 4.5 | 4.83 | 0.013 | 0.71 | 15.6 | 41.2 | 30.4 | 12.2 | 9.7 | 6.5 | 1.38 | 15.34 | 0.43 | 12021 | 13.3 | 21.3 | 62.7 | 2.3 | 18 | −27.8 | 68.9 |
| R2 | Innoko R. | 4.9 | 4.41 | 0.011 | 0.65 | 15.8 | 39.8 | 29.3 | 12.8 | 9.1 | 9.1 | 1.37 | 16.56 | 0.43 | 12200 | 16.7 | 22.9 | 56.7 | 3.4 | 14 | N/A | N/A |
| R3 | Forty Mile R. | 4.3 | 4.62 | 0.012 | 0.72 | 14.5 | 40.5 | 29.4 | 12.4 | 10.0 | 7.8 | 1.39 | 14.55 | 0.44 | 12664 | 15.5 | 21.0 | 59.1 | 4.0 | 15 | N/A | N/A |
| R4 | Yukon R. at Pilot, low Q | 2.8 | 6.53 | 0.016 | 0.79 | 15.1 | 41.0 | 27.2 | 8.4 | 13.9 | 9.5 | 1.54 | 10.95 | 0.56 | 9003 | 5.6 | 12.7 | 76.8 | 4.7 | 22 | −27.5 | −71.1 |
| P1 | NELHA, Pacific Ocean, 21 m | 0.6 | 14.19 | 0.028 | 1.57 | 1.5 | 32.5 | 18.8 | 5.7 | 41.3 | 1.8 | 1.57 | 1.08 | 0.94 | 5702 | 0.1 | 2.4 | 88.0 | 8.9 | 30 | −22.9 | −376.8 |
| P2 | NELHA, Pacific Ocean, 674 m | 0.9 | 4.86 | 0.015 | 1.74 | 4.24 | 35.5 | 25.9 | 14.6 | 15.5 | 8.6 | 1.53 | 6.11 | 0.65 | 4788 | 0.1 | 2.6 | 91.7 | 4.9 | 36 | −22.5 | −519.8 |
| G1 | Fremont | 2.8 | 6.42 | 0.017 | 0.92 | 9.8 | 37.5 | 23.7 | 9.2 | 18.7 | 10.9 | 1.40 | 5.16 | 0.55 | 9446 | 4.6 | 12.1 | 76.6 | 6.4 | 21 | N/A | N/A |
| L1 | Upper Lake Powell | 3.3 | 6.44 | 0.017 | 0.92 | 17.5 | 32.1 | 19.0 | 11.4 | 14.4 | 23.2 | 1.42 | 9.19 | 0.59 | 11124 | 5.6 | 11.6 | 74.7 | 7.6 | 21 | N/A | N/A |
| L2 | Lower Lake Powell | 2.3 | 9.44 | 0.022 | 1.10 | 8.5 | 29.6 | 16.8 | 8.2 | 22.4 | 23.1 | 1.44 | 4.25 | 0.71 | 8747 | 2.5 | 7.5 | 80.7 | 8.7 | 24 | N/A | N/A |
| G2 | Ohio R., low Q | 3.2 | 6.22 | 0.015 | 0.81 | 20.5 | 36.3 | 20.2 | 7.7 | 20.8 | 15.0 | 1.51 | 5.87 | 0.65 | 11050 | 4.9 | 12.3 | 76.1 | 6.3 | 18 | N/A | N/A |
| G3 | Ohio R., after peak Q | 3.6 | 5.37 | 0.013 | 0.71 | 22.7 | 39.1 | 24.1 | 9.7 | 14.4 | 12.7 | 1.50 | 9.69 | 0.55 | 10790 | 7.1 | 14.4 | 72.2 | 5.8 | 18 | N/A | N/A |
| G4 | Missouri R. | 2.8 | 8.05 | 0.019 | 0.94 | 16.0 | 30.6 | 18.4 | 10.9 | 16.2 | 23.8 | 1.43 | 7.28 | 0.63 | 9225 | 3.5 | 9.1 | 80.4 | 6.6 | 22 | N/A | N/A |
| A1 | Lake Hoare, 5.6 m | 1.7 | 9.93 | 0.023 | 1.23 | 6.0 | 36.7 | 19.2 | 7.0 | 27.8 | 9.3 | 1.63 | 3.16 | 0.81 | 9858 | 1.5 | 5.0 | 82.6 | 9.6 | 18 | N/A | N/A |
| A2 | Lake Fryxell FA, 5.5 m | 2.1 | 8.60 | 0.020 | 1.05 | 8.8 | 38.7 | 18.6 | 6.8 | 25.8 | 10.0 | 1.66 | 4.32 | 0.81 | 11204 | 2.0 | 5.9 | 82.4 | 8.5 | 18 | N/A | −7.9 |
| E | WCA-2b (Ever-glades) | 3.5 | 7.67 | 0.017 | 0.77 | 24.9 | 36.3 | 19.1 | 8.4 | 11.6 | 24.6 | 1.49 | 14.47 | 0.56 | 13618 | 6.8 | 15.0 | 73.1 | 4.6 | 20 | −26.6 | −60.5 |
| T | Cincinnati Tap Water | 1.9 | 9.64 | 0.018 | 0.82 | 8.1 | 44.4 | 23.3 | 6.3 | 21.8 | 4.2 | 1.59 | 5.92 | 0.72 | 8836 | 1.7 | 6.8 | 85.5 | 5.6 | 26 | N/A | N/A |
| R5 | Coal Creek | 4.5 | 5.02 | 0.013 | 0.71 | 18.7 | 39.1 | 26.2 | 12.7 | 10.8 | 11.1 | 1.35 | 10.46 | 0.45 | 14030 | 14.0 | 23.2 | 60.5 | 2.2 | 16 | N/A | N/A |



DOI: 10.1021/acs.est.7b05513
Environ. Sci. Technol. 2018, 52, 2538−2548

**Table 1. continued**

| NMDS label | site | $SUVA_{254}$ (L mg $C^{-1}$ $m^{-1}$) | $A_{250}/A_{365}$ | $S_{275-295}$ ($nm^{-1}$) | $S_R$ | $Fmax_{total}$ | % component 1 | % component 2 | % component 3 | % component 4 | % component 5 | fluorescence index (FI) | humification index (HIX) | biological index (BIX) | assigned formulas (#) | condensed aromatics (% RA) | polyphenolic (% RA) | unsaturated and phenolic (%RA) | aliphatic (%RA) | island of stability (IOS; % RA) | $\partial^{13}C$-DOC, ‰ | $\Delta^{14}C$-DOC, ‰ |
|---|---|---|---|---|---|---|---|---|---|---|---|---|---|---|---|---|---|---|---|---|---|---|
| R6 | Black R. | 4.6 | 4.36 | 0.012 | 0.72 | 14.8 | 40.8 | 27.4 | 12.1 | 10.3 | 9.5 | 1.40 | 13.55 | 0.44 | 11780 | 17.3 | 23.5 | 54.7 | 3.7 | 13 | −27.5 | 49.7 |
| R7 | Porcupine R. | 4.2 | 4.73 | 0.013 | 0.73 | 15.4 | 39.9 | 28.2 | 11.8 | 10.8 | 9.4 | 1.41 | 13.71 | 0.47 | 12169 | 13.0 | 19.8 | 62.9 | 3.8 | 16 | −27.5 | 39.2 |
| R8 | Koyakuk R. | 4.4 | 4.37 | 0.012 | 0.71 | 15.8 | 39.4 | 29.2 | 12.4 | 10.8 | 8.2 | 1.41 | 13.00 | 0.45 | 11679 | 18.8 | 23.4 | 53.1 | 4.3 | 12 | N/A | N/A |
| R9 | Yukon R. at Eagle | 3.3 | 5.81 | 0.015 | 0.82 | 13.1 | 38.7 | 24.9 | 10.3 | 13.8 | 12.3 | 1.41 | 10.05 | 0.53 | 10022 | 8.5 | 15.5 | 72.7 | 3.0 | 22 | −26.8 | 13.7 |
| R10 | White R. | 3.4 | 5.53 | 0.015 | 0.81 | 15.7 | 39.0 | 26.4 | 10.1 | 13.6 | 10.9 | 1.46 | 10.55 | 0.53 | 10125 | 7.5 | 14.9 | 73.7 | 3.7 | 22 | −26.9 | −1.1 |
| R11 | Yukon R. at Pilot, peak Q | 3.9 | 4.65 | 0.012 | 0.73 | 14.6 | 40.4 | 27.6 | 10.6 | 13.1 | 8.4 | 1.46 | 8.82 | 0.49 | 11951 | 12.1 | 18.3 | 62.3 | 6.6 | 14 | −28.1 | 92.2 |
| R12 | Yukon R. at Pilot, after peak Q | 4.3 | 4.71 | 0.012 | 0.72 | 14.8 | 40.7 | 28.3 | 11.0 | 11.2 | 8.9 | 1.40 | 11.40 | 0.46 | 11834 | 14.6 | 20.5 | 59.4 | 5.0 | 13 | −28.1 | 82.1 |
| G5 | Aquifer (Colorado R., Rifle) | 1.8 | 8.67 | 0.017 | 0.76 | 13.8 | 36.6 | 19.9 | 7.8 | 15.9 | 19.8 | 1.62 | 11.49 | 0.69 | 4086 | 0.8 | 5.3 | 90.6 | 3.3 | 36 | N/A | N/A |
| L3 | Shingobee Lake | 3.3 | 7.06 | 0.018 | 0.89 | 13.4 | 34.4 | 19.0 | 7.7 | 19.0 | 19.9 | 1.47 | 6.08 | 0.65 | 11062 | 4.8 | 11.7 | 76.5 | 6.6 | 22 | −29.1 | −45.7 |
| L4 | Williams Lake | 2.0 | 8.26 | 0.020 | 1.05 | 6.8 | 35.6 | 20.1 | 7.4 | 24.8 | 12.1 | 1.50 | 3.17 | 0.72 | 10441 | 1.8 | 6.1 | 80.0 | 11.3 | 21 | −26.1 | 69.7 |
| G6 | Biscayne Bay | 3.9 | 6.55 | 0.016 | 0.80 | 31.9 | 36.2 | 20.3 | 10.4 | 10.4 | 22.5 | 1.46 | 18.28 | 0.54 | 11793 | 6.6 | 15.8 | 74.6 | 2.9 | 23 | −28 | −63.6 |
| G7 | Laramie Fox-Hills Aquifer | 1.7 | 12.87 | 0.025 | 1.03 | 23.7 | 37.9 | 14.1 | 2.1 | 31.6 | 14.3 | 1.89 | 4.02 | 1.03 | 7581 | 0.6 | 7.4 | 86.1 | 5.1 | 21 | −24.3 | N/A |
| S1 | Penobscot R. at Eddington | 4.5 | 4.66 | 0.013 | 0.73 | 11.9 | 40.2 | 28.7 | 12.3 | 10.9 | 7.9 | 1.34 | 11.79 | 0.45 | 11625 | 16.2 | 24.8 | 56.0 | 2.8 | 15 | −27.6 | 72.8 |
| S2 | Penobscot Bay | 3.1 | 5.31 | 0.015 | 0.90 | 9.1 | 35.6 | 22.2 | 9.8 | 17.8 | 14.7 | 1.39 | 5.56 | 0.56 | 9568 | 5.7 | 11.7 | 76.2 | 5.9 | 25 | −25.3 | −65.9 |
| S3 | Gulf of Maine | 1.8 | 6.87 | 0.018 | 1.02 | 6.6 | 34.1 | 20.7 | 8.6 | 23.2 | 13.5 | 1.45 | 3.66 | 0.68 | 6985 | 1.7 | 5.3 | 88.0 | 4.8 | 33 | −24.3 | −215.6 |
| P3 | Pacific Ocean, 240 m | 0.7 | 10.78 | 0.022 | 1.27 | 2.5 | 31.8 | 17.7 | 5.5 | 44.5 | 0.5 | 1.56 | 1.05 | 0.98 | 5580 | 0.1 | 2.0 | 92.5 | 5.1 | 38 | −23 | −401.1 |
| R13 | Suwannee R.[b] | 4.6 | 4.46 | 0.012 | 0.65 | 14.7 | 39.2 | 30.8 | 14.1 | 7.1 | 8.8 | 1.33 | 21.33 | 0.39 | 10797 | 15.1 | 23.1 | 59.4 | 2.2 | 19 | −27.7 | 58.4 |
| NOM1 | Nordic Reservoir[b], 10 m | 4.1 | 4.66 | 0.013 | 0.76 | 10.7 | 43.5 | 30.5 | 10.7 | 9.5 | 5.8 | 1.42 | 15.78 | 0.44 | 13925 | 10.7 | 18.8 | 64.8 | 4.4 | 17 | −27.8 | 170 |



DOI: 10.1021/acs.est.7b05513
Environ. Sci. Technol. 2018, 52, 2538−2548

Table 1. continued

| NMDS label | site | $SUVA_{254}$ (L mg $C^{-1}$ $m^{-1}$) | $A_{250}/A_{365}$ | $S_{275-295}$ ($nm^{-1}$) | $S_R$ | $Fmax_{total}$ | % component 1 | % component 2 | % component 3 | % component 4 | % component 5 | fluorescence index (FI) | humification index (HIX) | biological index (BIX) | assigned formulas (#) | condensed aromatics (% RA) | polyphenolic (% RA) | unsaturated and phenolic (%RA) | aliphatic (%RA) | island of stability (IOS; % RA) | $\partial^{13}C$-DOC, ‰ | $\Delta^{14}C$-DOC, ‰ |
|---|---|---|---|---|---|---|---|---|---|---|---|---|---|---|---|---|---|---|---|---|---|---|
| NOM2 | Upper Mississippi R.[b] | 3.6 | 5.16 | 0.015 | 0.86 | 14.1 | 41.4 | 27.1 | 11.1 | 12.0 | 8.4 | 1.48 | 13.14 | 0.54 | 16552 | 10.8 | 19.7 | 64.9 | 2.1 | 14 | N/A | N/A |
| A3 | Pony Lake[b] | 2.8 | 4.81 | 0.013 | 0.77 | 13.3 | 40.0 | 27.7 | 11.1 | 21.2 | 0.0 | 1.56 | 6.73 | 0.77 | 11808 | 2.2 | 6.2 | 74.2 | 13.3 | 11 | N/A | N/A |

[a]NMDS: nonmetric multidimensional scaling; $SUVA_{254}$: carbon specific UV absorbance at 254 nm; $A_{250}/A_{365}$: ratio of absorbance at 250 and 365 nm; $S_{275-295}$: spectral slope between 275 and 295 nm; $S_R$: spectral ratio; $Fmax_{total}$: sum of fluorescence component maximum intensities; %RA: percent of the relative abundance; R.: River; Q: discharge; N/A: data not available. [b]Denotes samples acquired from International Humic Substances Society. All others were collected and isolated by G. R. Aiken and colleagues between 1979 and 2015.

to the sum of the Fmax values were calculated for each component and are reported as percent component C1−C5 (%C1−%C5; Table 1).

**FT-ICR MS.** Solid DOM isolates were redissolved in Milli-Q and combined to a final ratio of 30% Milli-Q and 70% methanol, containing 40 mg C $L^{-1}$ of DOM. Extracts were stored at 4 °C prior to analysis on a custom-built 9.4-T FT-ICR mass spectrometer with a 22 cm diameter bore at the National High Magnetic Field Laboratory (Tallahassee, FL).[37] Negatively charged ions of DOM were produced via electrospray ionization at a flow rate of 700 nL $min^{-1}$ and collected over 100 conditionally coadded scans.

Molecular formulas were assigned to peaks with intensity >6$\sigma$ RMS baseline noise based on published rules[38] using an in-house software (EnviroOrg[39]) developed at the National High Magnetic Field Laboratory within the bounds of $C_{1-45}H_{1-92}N_{0-4}O_{1-25}S_{0-2}$. The mass error did not exceed 300 ppb. The modified aromaticity index ($AI_{mod}$) was calculated to determine the degree of unsaturation based on the molecular formula.[40] Compound categories were defined as follows: condensed or polycyclic aromatic ($AI_{mod} > 0.66$), polyphenolic ($0.66 \geq AI_{mod} > 0.5$), highly unsaturated and phenolic (AImod <0.5 and H/C < 1.5), aliphatic ($2 \geq H/C \geq 1.5$, $N = 0$), peptide-like ($2 \geq H/C \geq 1.5$, $N > 0$), or sugar-like ($O/C > 0.9$).[3,41] The compound categories peptide-like and sugar-like are based on similarities in elemental composition and together make up less than 1.5% of the relative abundance of any sample with the exception of the Upper Mississippi NOM, which was high in sugar-like compounds (2.5% relative abundance), and Pony Lake FA, which was high in peptide-like compounds (4.0% relative abundance). Although FT-ICR MS allows for the precise assignment of molecular formulas to peaks which may represent multiple isomers, they describe the underlying molecular compounds comprising DOM, thus throughout the paper, the term compound may be used when discussing the peaks detected by FT-ICR MS.

**Dissolved Organic Carbon Stable and Radiocarbon Isotopic Analyses.** Stable carbon isotopes and radiocarbon were analyzed according to previously described methods.[42] Briefly, inorganic carbon was removed by sparging acidified samples (0.2 mL of 40% phosphoric acid) with nitrogen. Samples were subsequently sparged with $O_2$ before UV oxidation. The produced $CO_2$ was cryogenically purified in a vacuum line, converted to graphite targets using an iron catalyst under 1 atm $H_2$ at 550 °C, and analyzed for $\delta^{13}$C-DOC and $\Delta^{14}$C-DOC at the National Ocean Sciences Accelerator Mass Spectrometry (NOSAMS) facility at the Woods Hole Oceanographic Institution and the University of Arizona's AMS facility. $\Delta^{14}$C data (in ‰) were corrected for isotopic fractionation using measured $\delta^{13}$C values.

**Data Management and Statistical Analyses.** All data generated or analyzed during this study are included in the main text or SI of this publication. PARAFAC modeling, calculation of optical indices and fluorescence plots were conducted in Matlab, using the drEEM toolbox.[35] Multivariate, linear and nonlinear modeling and remaining graphing were conducted in base R[43] along with the packages vegan[44] and Hmisc.[45] *P*-values were adjusted for multiple comparisons using the false discovery rate correction[46] in R. A false discovery rate adjusted *p*-value < 0.05 is considered significant

## RESULTS AND DISCUSSION

Samples covered a wide spectrum of DOM molecular composition, encompassing modern, highly aromatic allochthonous



DOI: 10.1021/acs.est.7b05513
Environ. Sci. Technol. 2018, 52, 2538−2548

DOM, to aged DOM with low aromaticity, dominated by autochthonous production (Table 1). Our analysis of DOM isolates from groundwaters, rivers, lakes and marine waters supports previous regional studies[3,12,13,24] by showing that the relationships between highly aromatic, polyphenolic, and polycyclic compounds, and optical properties associated with allochthonous DOM, such as elevated $SUVA_{254}$ and long-wavelength emission fluorescence components, were consistent across the full spectrum of aquatic ecosystems. Likewise, DOM in oceanic and lake ecosystems with limited relative allochthonous inputs had a higher fraction of aliphatic compounds and compounds with H/C > 1, and optical properties typical of autochthonous DOM[14,18] (Table 1, SI Table 3). Additionally, we illustrate that aging results in the distinct chemical composition of DOM from sites historically considered autochthonous microbial endmembers: recently produced DOM in Antarctic lakes versus aged DOM from the deep Pacific Ocean.

**Gradients between Optical Properties of Allochthonous and Autochthonous Sources of DOM.** $SUVA_{254}$ ranged from 0.6 to 4.9 L mg $C^{-1}$ $m^{-1}$ (mean: 3.1 L mg $C^{-1}$ $m^{-1}$). The highest values were observed in rivers with a strong influence from the catchment (Alaskan rivers, Suwannee River, and Penobscot River; Table 1). Lower $SUVA_{254}$ values were observed in groundwater and the Pacific Ocean. Similarly, $A_{250}/A_{365}$ (mean: 6.7; range: 4.4−14.2), $S_R$ (mean: 0.89; range: 0.65−1.74), and $S_{275-295}$ (mean: 0.016 $nm^{-1}$; range: 0.011−0.028 $nm^{-1}$) had low or shallow values in systems with a strong influence from the catchment and high $SUVA_{254}$ values (Table 1). Fluorescence analyses showed similar trends, which largely reflects decreasing aromaticity, with low HIX (mean: 9.39; range: 1.05−21.33), high FI (mean: 1.48; range: 1.33−1.89), and high BIX (mean: 0.60; range: 0.39−1.03) in the Pacific Ocean, large lakes, and river samples (Table 1).

PARAFAC analysis validated five fluorescence components (SI Figure 1), all of which have been described previously.[36] Components matched between 5 and 15 components previously uploaded to OpenFluor with a minimum similarity score of 0.95 from PARAFAC models validated for DOM in a wide variety of systems: component 1 (C1)—15 matches; C2—11 matches, C3—7 matches, C4—5 matches, C5—12 matches. These ranged from studies of DOM across the world including boreal lakes, alpine streams, tropical rivers, and the ocean. All PARAFAC components were red-shifted, which is expected of the extractions targeting the hydrophobic organic acid (HPOA; $n$ = 22) and fulvic acid (FA; $n$ = 13) fractions of DOM that form the majority of this data set (examples of excitation−emission matrices are given in SI Figure 3). Component 1 is similar to classically described microbial-humic fluorescence with an excitation maximum <260 nm (secondary at 315 nm), and an emission maximum at 423 nm. Components 2 (ex: < 260 (345); em: 476) and 3 (ex: 270 (435); em: 544) are typical of red-shifted fluorescence, reminiscent of humic and soil-derived fluorescence. Component 4 (ex: < 260 (290); em: 377) is similar to what is classically described as tryptophan-like fluorescence, and component 5 (ex: 260; em: 439) is similar to classical peak A[18]. There was a second, shorter emission wavelength protein-like peak in the residuals of the Pacific Ocean samples and the Laramie Fox-Hills groundwater sample that could not be validated. The percent contribution of components 1−3 to total fluorescence (%C1−%C3) was elevated in systems with high $SUVA_{254}$ values and a strong connection to the catchment. The relative contribution of component 4 (%C4) was highest in the Pacific Ocean samples at 240 and 21 m, and the Laramie Fox-Hills groundwater sample (Table 1). The intensity of components 1−3 and component 5 are broadly related to the percent contribution of the respective components, for example, C1 is weakly, yet significantly related to %C1 (Table 1; C1 v. %C1: $R^2$ = 0.13, $p$-value = 0.03; C2 v. %C2: $R^2$ = 0.26, $p$-value = 0.001; C3 v. %C3: $R^2$ = 0.40, $p$-value <0.0001; C5 v. %C5: $R^2$ = 0.68, $p$-value <0.0001). C1−C3 and %C1−%C3 are elevated at sites with high $SUVA_{254}$ and polyphenolic and condensed aromatic compounds. C4 and %C4 are not correlated, as %C4 reaches maximum values in the Pacific Ocean samples, but the maximum C4 value is observed in samples with an intermediate $SUVA_{254}$.

**Molecular DOM Composition and Associations with Optical Properties.** The FT-ICR MS data showed that samples were relatively enriched in condensed or polycyclic aromatic compounds (mean relative abundance: 7.4%; range: 0.1−18.8%; Table 1) and polyphenolic compounds (mean: 13.5%; range: 2.0−24.7%), with the majority of the relative abundance composed of highly unsaturated and phenolic compounds (mean: 73.0%; range: 53.1−92.5%). A smaller proportion of the relative abundance was of aliphatic compounds (mean: 5.4%; range: 2.1−13.3%), peptide-like (mean: 0.4%; range: 0.0−4.0%) and sugar-like compounds (mean: 0.2%; range: 0.0−1.7%; Table 1 and SI Table 3). The high range observed within compound groups, particularly in condensed and polycyclic aromatics and polyphenolic compounds, is consistent with the large range of $SUVA_{254}$ values and the extremely red-shifted fluorescence observed. Samples with high contributions from condensed and polycyclic aromatics and polyphenolic compounds were samples with DOM from allochthonous sources. Samples with low contributions from polycyclic aromatics and polyphenolic compounds generally exhibited higher contributions from aliphatic compounds and peptide-like compounds, such as samples with DOM from predominantly autochthonous sources.

A nonmetric multidimensional scaling (NMDS, stress = 0.046, $k$ = 3) based on FT-ICR MS derived molecular composition showed a clear separation between highly aromatic, allochthonous-dominated riverine samples on the negative end of the first dimension (NMDS1) with Pacific Ocean samples on the positive end (Figure 2, Table 1 and SI Table 1 and 3). The input parameters for the ordination include the percent relative abundance of condensed aromatic compounds, polyphenolic compounds, highly unsaturated and phenolic compounds (HUPs), aliphatic compounds, and peptide-like compounds; the total number of assigned formulas (#Formula); the percent of assigned formulas identified as CHO, CHON, CHOS, or CHONS; and the relative intensity weighted averages of mass (i.e., $m/z$ where $z$ = 1), $AI_{mod}$, the nominal oxidation state of carbon (NOSC), H/C, O/C, and N/C. $SUVA_{254}$, humification index, and PARAFAC derived components %C1, %C2, and %C3 highly covaried with riverine samples with a high proportion of polyphenolic and condensed aromatic compounds (Figure 2b). Conversely, biological index, fluorescence index, spectral slope ratio ($S_R$), absorbance ratio ($A_{250}/A_{365}$), spectral slope ($S_{275-295}$), and %C4 were positively related with the first dimension and samples that were less aromatic and dominated by autochthonous inputs, such as the Pacific Ocean and Antarctic lake samples (Figure 2b). The separation of highly aromatic, long emission fluorescence with high contributions from polyphenolic compounds versus aliphatic, short emission fluorescence across DOM from all types of aquatic systems in diverse biomes strengthens past findings from regional studies.[3,26] Biological and humification indices also separate along the second dimension of the NMDS but not as


DOI: 10.1021/acs.est.7b05513
Environ. Sci. Technol. 2018, 52, 2538−2548

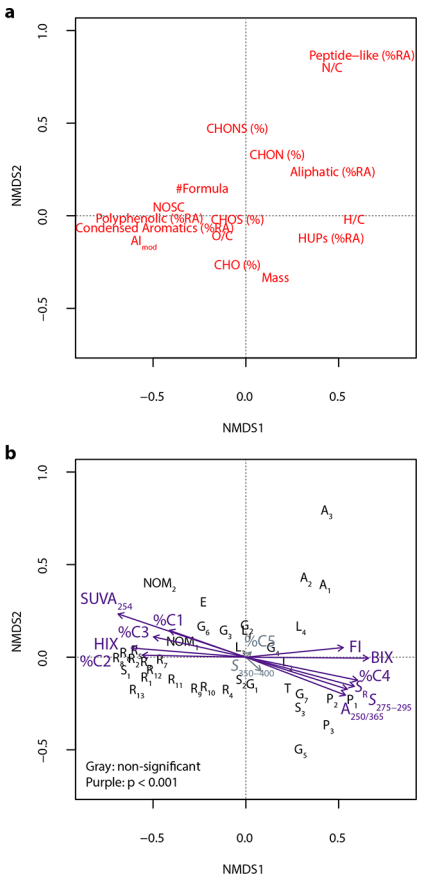



**Figure 2.** Multivariate analysis of molecular composition using nonmetric multidimensional scaling. (a) The ordination was based on Bray−Curtis dissimilarities of 16 variables derived from FT-ICR MS molecular composition ($k$ = 3, stress = 0.046). (b) Optical indices were fit to the same ordination over 999 permutations, with the color indicating the significance level: not significant (gray) and $p$-value < 0.001 (purple). Black labels indicate samples detailed in Table 1 and SI Table 1 and 3. Other abbreviations: $SUVA_{254}$ (carbon specific UV absorbance at 254 nm); HIX (humification index); %C1−%C5 (percent contribution from PARAFAC components); BIX (biological index); FI (fluorescence index); $S_R$ (spectral slope ratio); $A_{250}/A_{365}$ (absorbance ratio); and $S_{275-295}$ and $S_{350-400}$ (spectral slope from 275 to 295 nm and from 350−400 nm).

strongly as they do along the first axis (NMDS2; Figure 2b). This suggests that the second dimension reflects recent autochthonous production, which is supported by the high scores on NMDS2 of the weighted average of N/C, the percent of compounds containing N, and the percent relative abundance of peptide-like compounds (Figure 2a).

The intensity-weighted average of the FT-ICR MS derived modified aromaticity index ($AI_{mod}$) has a significant semilog relationship with $SUVA_{254}$ ($R^2$ = 0.88, $p$-value < 0.001; Figure 3a), however, the percent contribution from polycyclic and polyphenolic compounds shows an even tighter, but exponential relationship with $SUVA_{254}$, saturating at 5.0 L mg $C^{-1}$ $m^{-1}$ ($R^2$ = 0.95, $p$-value < 0.001; Figure 3b). This suggests that even if the percent relative abundance of polycyclic and polyphenolic compounds continues to increase, a concurrent increase in $SUVA_{254}$ will not be observed. This is consistent with findings over the past decades where reports of samples from natural aquatic systems reporting $SUVA_{254}$ above 5.5 are rare, and likely have not accounted for absorbance from iron or other interfering constituents.[14,47,48] The fraction of molecular carbon that can be tied up in aromatic structures is limited in DOM as aromatic structures are nonpolar and require functionalized side chains to remain in solution, suggesting the upper limit of $SUVA_{254}$ for DOM in aquatic systems is due to solubility constraints.

The significant positive relationship between $SUVA_{254}$ and the percent relative abundance of polycyclic aromatics and polyphenolic compounds is further reflected in the molecular-level relationships between $SUVA_{254}$ and FT-ICR MS detected compounds (SI Figure 4). Compounds significantly positively related with $SUVA_{254}$ ($n$ = 6621) were mostly condensed or polyphenolic aromatic compounds (69%). Conversely, compounds significantly positively correlated with the biological index are almost entirely highly unsaturated and phenolic compounds, aliphatic compounds, or peptide-like compounds (97%). N-containing compounds account for 53%, including the 131 compounds most strongly associated with the biological index (where Spearman's rho >0.88). This highlights the utility of simple optical measurements for assessing DOM composition across the full spectrum of aquatic ecosystems.

**Isotopic Evidence for a Modern, Terrestrial Source of Condensed Aromatic Compounds.** The increase in the relative abundance of polyphenolic and condensed aromatic compounds with increasing $SUVA_{254}$ supports previous findings that show high $SUVA_{254}$ values reflect DOM from allochthonous sources. The terrestrial source of polycyclic and polyphenolic compounds is further supported by the significant relationship between these compounds and depleted $\delta^{13}$C-DOC ($R^2$ = 0.84, $p$-value < 0.01; Figure 3c). $\Delta^{14}$C-DOC has a saturating positive relationship with polycyclic aromatic compounds ($R^2$ = 0.81, $p$-value < 0.05; Figure 3d). Thus, samples with higher contributions from polycyclic aromatic compounds have a modern DOM source, which suggests rapid mobilization from the catchment. Globally, rivers export combustion-derived polycyclic aromatic compounds from catchments to the ocean at an average ± SD of 7.1 ± 3.6% of DOC concentration.[49] The enriched $\Delta^{14}$C-DOC values for samples with over 12% of the relative abundance from polycyclic aromatics in the current study (mean ± s.e.: 66 ± 7‰, $n$ = 7) seem to preclude them from having a fossil source. Therefore, either there is a stock of modern fire-derived polycyclic aromatic compounds that is relatively universal and proportional to the DOM produced in any given system, or polycyclic aromatic compounds may be produced in the absence of combustion on the terrestrial landscape, potentially via humification processes.[50] At the other end of the spectrum, the relative abundance of polycyclic aromatic compounds in the Pacific Ocean samples approaches but does not quite reach zero, in accordance with previous studies that have measured limited dissolved black carbon in the ocean.[51]

**Compositional Progression from Modern, Terrestrial DOM to Aged, Persistent DOM.** The abundance of polycyclic aromatic compounds in systems with high connectivity to the catchment is illustrated by the DOM composition in the Yukon River at Pilot Station at peak discharge (i.e., low H/C and low O/C, Figure 4a; Table 1). The percent relative abundance of polycyclic aromatic compounds decreases from 12.1% in the Yukon River at Pilot Station to 2.0% in Lake Fryxell, Antarctica (Figure 4b) and 0.1% in the Pacific Ocean deep DOM (Figure 4c). In addition to the decreased contribution from polycyclic aromatic compounds (1−2 orders of magnitude), the autochthonous end-members (Lake Fryxell versus Pacific Ocean deep water) are distinct from one another in chemical composition. First, $SUVA_{254}$ in Lake Fryxell is twice as high as in the Pacific Ocean deep water (see Table 1). Second, Lake


DOI: 10.1021/acs.est.7b05513
Environ. Sci. Technol. 2018, 52, 2538−2548

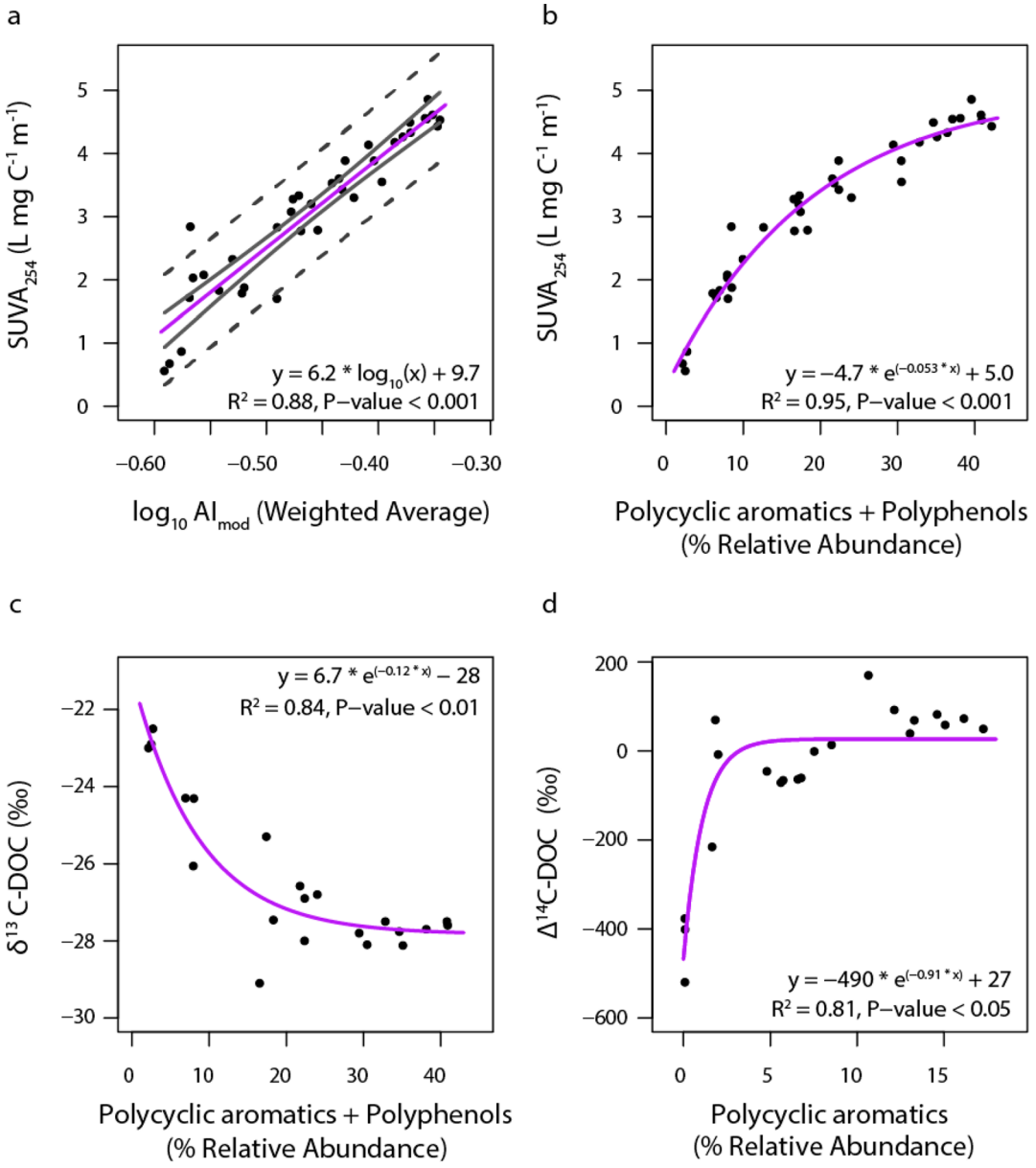



**Figure 3.** Relationships between molecular composition, optical properties and isotopic content. Changes in $SUVA_{254}$ against (a) $\log_{10}$ transformed modified aromaticity index and (b) percent relative abundance of polycyclic and polyphenolic aromatic compounds ($n$ = 37), and changes in isotopic composition against molecular composition; (c) $\delta^{13}$C-DOC against percent relative abundance of polycyclic and polyphenolic aromatic compounds and (d) $\Delta^{14}$C-DOC against polycyclic aromatic compounds ($n$ = 21).

Fryxell maintains a high molecular richness, with 11 204 molecular formulas assigned, similar to the 11 951 formulas assigned in the Yukon River; whereas approximately 4788 formulas were assigned in the deep Pacific Ocean. The fraction of CHON compounds increases by 20% in Lake Fryxell and only 4% in the deep Pacific, in comparison to the Yukon River at Pilot Station. Finally, the percent relative abundance of compounds that are part of the IOS increases from the Yukon River at Pilot Station (14%), to Lake Fryxell (18%) to the deep Pacific Ocean (35%). That is, as the age of the DOC increases, the relative abundance of the IOS increases proportionally (Figure 4d). The coupling between age and IOS is evident among all samples for which $\Delta^{14}$C-DOC data is available ($n$ = 21; $R^2$ = 0.82, $p$-value < 0.001; Figure 4d). The compounds that make up the IOS have previously been suggested as those compounds that are most strongly correlated to depleted $\Delta^{14}$C-DOC in a DOM study from the Atlantic Ocean[4] and fall within the bounds of carboxylic-rich alicyclic molecules, which have been suggested as a group of potentially recalcitrant organic compounds in marine systems.[52] This study shows that the association between age and composition holds across allochthonous to autochthonous end-members, not only within aged DOM in the ocean. This loss of modern, aromatic DOM, as well as a significant decrease in the molecular richness from modern DOM (both allochthonous and autochthonous), signals a strong control of time on molecular composition leading to the formation of a narrow range of degradation products, or compounds that resist degradation and ultimately persist in the deep ocean.

**Time Results in Divergent Composition between Autochthonous End-Members.** Antarctic lakes and the Pacific Ocean are considered end-members of autochthonously sourced DOM.[27,53,54] However, there are stark compositional differences



DOI: 10.1021/acs.est.7b05513
Environ. Sci. Technol. 2018, 52, 2538–2548

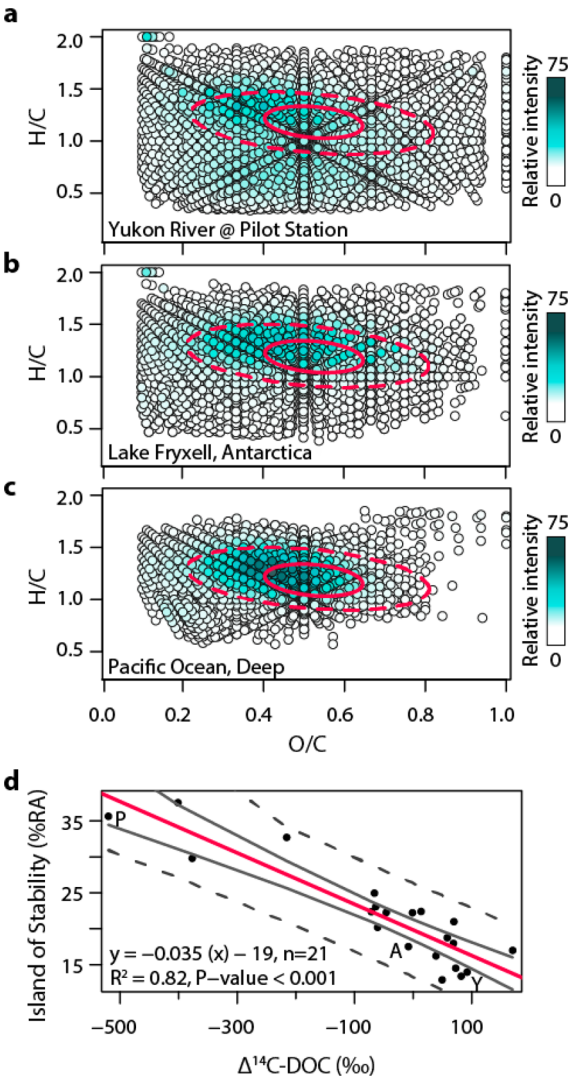



**Figure 4.** Progression of DOM composition over time. Panels (a, b, c) show the shift in molecular composition from a system with modern (Y = Yukon River at Pilot Station), intermediate (A = Lake Fryxell, Antarctica), and old DOC (*P* = deep Pacific Ocean, 674 m). Panel (d) shows the relationship between the percent relative abundance of the "island of stability" against $\Delta^{14}$C-DOC. The inner solid circle in (a, b, c) is the average and standard deviation of the elemental composition of the IOS.[4] The outer dashed circle encompasses all compounds included in the IOS. Both circles are plotted for reference, but the actual bounds may vary slightly.

between the two, with DOM from the Antarctic lakes exhibiting modern $\Delta^{14}$C-DOC and higher molecular richness (i.e., chemodiversity) including a plethora of N-containing compounds. DOM in Antarctic lakes originates from algae and bacteria, such as cyanobacteria,[53] and despite an intermediate $SUVA_{254}$ value there are no sources of terrestrial organic matter in the catchment, where the soils have an organic content of <0.1%.[55] Alternatively, DOM in the Pacific Ocean is highly photochemically and microbially degraded, thus it is an aged mixture of compounds produced by photosynthesis in the surface oceans[56] and may contain remnants of highly degraded DOM from allochthonous inputs, as vast quantities of DOM are delivered to the ocean.[57,58] Both types of systems contain DOM that originates from predominantly autochthonous sources, however, this study shows the extreme differentiation in DOM composition and diversity that results from differences in extent of degradation, suggesting time is not only a driver of degradation,[7] but also a dominant control over DOM molecular composition and diversity across aquatic ecosystems.

## ■ ASSOCIATED CONTENT

### Supporting Information

The Supporting Information is available free of charge on the ACS Publications website at DOI: 10.1021/acs.est.7b05513.

Loadings of PARAFAC components (Supplementary Figure 1), split-half analysis of PARAFAC components (Supplementary Figure 2), examples of excitation−emission matrices (Supplementary Figure 3), Van Krevelen diagrams of molecular relationships with $SUVA_{254}$ and biological index (Supplementary Figure 4), sample names, site types, and coordinates (Supplementary Table 1), loadings of PARAFAC components (Supplementary Table 2), and additional data that were used in the multivariate ordination (NMDS; Supplementary Table 3) (PDF)

## ■ AUTHOR INFORMATION


### Corresponding Author

*E-mail: akellerman@fsu.edu.

### ORCID

Anne M. Kellerman: 0000-0002-7348-4814

### Present Addresses

[‖]Now at Research Center for Watershed - Aquatic Ecosystem Interactions (RIVE), Université du Québec à Trois-Rivières, Trois-Rivières, Québec, Canada.

[‡]Pontchartrain Institute for Environmental Sciences, Department of Chemistry, University of New Orleans, New Orleans, Louisiana 70148, United States


### Author Contributions

G.R.A. collected the isolates over the past four decades alongside K.D.B. A.M.K., R.G.M.S., and G.R.A. conceived the study and selected the study sites. A.M.K. ran the optical and mass spectrometric analyses with significant assistance from F.G. and D.C.P. A.M.K. conducted the statistical analyses and wrote the manuscript with comments and suggestions from R.G.M.S. All authors commented on the manuscript.

### Notes

The authors declare no competing financial interest.

## ■ ACKNOWLEDGMENTS


George Aiken passed away in December 2016, as this manuscript was being prepared. The legacy he leaves behind cannot be measured solely by the quality of his science but more importantly by those he mentored along the way. All authors are eternally grateful to have been his colleague and his friend. We thank S.E. Johnston and P. Zito for help with sample preparation and data processing and Greg Fiske for making the base map. This research was supported by grants to R.G.M.S. from the National Science Foundation (Grant#: ANT 1203885, OCE 1333157, OCE 1464396, PLR 1500169) and supported by the U.S. Geological Survey National Stream Quality Accounting Network (http://water.usgs.gov/nasqan) and the U.S. Geological Survey National Research Program (http://water.usgs.gov/nrp). The National High Magnetic Field Laboratory is funded by the National Science Foundation (DMR 11-57490). F. Guillemette was partly supported by a postdoctoral fellowship from the Fond de Recherche du Québec − Nature et Technologies. The use of brand names in this report is for identification purposes




DOI: 10.1021/acs.est.7b05513
*Environ. Sci. Technol.* 2018, 52, 2538−2548

only and does not imply endorsement by the U.S. Geological Survey.

## REFERENCES


(1) Schmidt, M. W.; Torn, M. S.; Abiven, S.; Dittmar, T.; Guggenberger, G.; Janssens, I. A.; Kleber, M.; Kogel-Knabner, I.; Lehmann, J.; Manning, D. A.; Nannipieri, P.; Rasse, D. P.; Weiner, S.; Trumbore, S. E. Persistence of soil organic matter as an ecosystem property. *Nature* **2011**, *478* (7367), 49−56.

(2) Lehmann, J.; Kleber, M. The contentious nature of soil organic matter. *Nature* **2015**, *528* (7580), 60−8.

(3) Kellerman, A. M.; Kothawala, D. N.; Dittmar, T.; Tranvik, L. J. Persistence of dissolved organic matter in lakes related to its molecular characteristics. *Nat. Geosci.* **2015**, *8* (6), 454−457.

(4) Lechtenfeld, O. J.; Kattner, G.; Flerus, R.; McCallister, S. L.; Schmitt-Kopplin, P.; Koch, B. P. Molecular transformation and degradation of refractory dissolved organic matter in the Atlantic and Southern Ocean. *Geochim. Cosmochim. Acta* **2014**, *126*, 321−337.

(5) Arrieta, J. M.; Mayol, E.; Hansman, R. L.; Herndl, G. J.; Dittmar, T.; Duarte, C. M. Dilution limits dissolved organic carbon utilization in the deep ocean. *Science* **2015**, *348* (6232), 331−3.

(6) Flerus, R.; Lechtenfeld, O. J.; Koch, B. P.; McCallister, S. L.; Schmitt-Kopplin, P.; Benner, R.; Kaiser, K.; Kattner, G. A molecular perspective on the ageing of marine dissolved organic matter. *Biogeosciences* **2012**, *9* (6), 1935−1955.

(7) Catalán, N.; Marcé, R.; Kothawala, D. N.; Tranvik, L. J. Organic carbon decomposition rates controlled by water retention time across inland waters. *Nat. Geosci.* **2016**, *9* (7), 501−504.

(8) Sun, L.; Perdue, E. M.; Meyer, J. L.; Weis, J. Use of elemental composition to predict bioavailability of dissolved organic matter in a Georgia river. *Limnol. Oceanogr.* **1997**, *42* (4), 714−721.

(9) Stubbins, A.; Spencer, R. G. M.; Chen, H.; Hatcher, P. G.; Mopper, K.; Hernes, P. J.; Mwamba, V. L.; Mangangu, A. M.; Wabakanghanzi, J. N.; Six, J. Illuminated darkness: Molecular signatures of Congo River dissolved organic matter and its photochemical alteration as revealed by ultrahigh precision mass spectrometry. *Limnol. Oceanogr.* **2010**, *55* (4), 1467−1477.

(10) Riedel, T.; Biester, H.; Dittmar, T. Molecular fractionation of dissolved organic matter with metal salts. *Environ. Sci. Technol.* **2012**, *46* (8), 4419−26.

(11) Mopper, K.; Stubbins, A.; Ritchie, J. D.; Bialk, H. M.; Hatcher, P. G. Advanced instrumental approaches for characterization of marine dissolved organic matter: Extraction techniques, mass spectrometry, and nuclear magnetic resonance spectroscopy. *Chem. Rev.* **2007**, *107* (2), 419−442.

(12) Stubbins, A.; Lapierre, J. F.; Berggren, M.; Prairie, Y. T.; Dittmar, T.; del Giorgio, P. A. What's in an EEM? Molecular signatures associated with dissolved organic fluorescence in boreal Canada. *Environ. Sci. Technol.* **2014**, *48* (18), 10598−606.

(13) Herzsprung, P.; von Tumpling, W.; Hertkorn, N.; Harir, M.; Buttner, O.; Bravidor, J.; Friese, K.; Schmitt-Kopplin, P. Variations of DOM Quality in Inflows of a Drinking Water Reservoir: Linking of van Krevelen Diagrams with EEMF Spectra by Rank Correlation. *Environ. Sci. Technol.* **2012**, *46* (10), 5511−5518.

(14) Weishaar, J. L.; Aiken, G. R.; Bergamaschi, B. A.; Fram, M. S.; Fujii, R.; Mopper, K. Evaluation of specific ultraviolet absorbance as an indicator of the chemical composition and reactivity of dissolved organic carbon. *Environ. Sci. Technol.* **2003**, *37* (20), 4702−4708.

(15) Del Vecchio, R.; Blough, N. V. On the origin of the optical properties of humic substances. *Environ. Sci. Technol.* **2004**, *38* (14), 3885−91.

(16) Helms, J. R.; Stubbins, A.; Ritchie, J. D.; Minor, E. C.; Kieber, D. J.; Mopper, K. Absorption spectral slopes and slope ratios as indicators of molecular weight, source, and photobleaching of chromophoric dissolved organic matter. *Limnol. Oceanogr.* **2008**, *53* (3), 955−969.

(17) Wilson, H. F.; Xenopoulos, M. A. Effects of agricultural land use on the composition of fluvial dissolved organic matter. *Nat. Geosci.* **2009**, *2* (1), 37−41.

(18) Fellman, J. B.; Hood, E.; Spencer, R. G. M. Fluorescence spectroscopy opens new windows into dissolved organic matter dynamics in freshwater ecosystems: A review. *Limnol. Oceanogr.* **2010**, *55* (6), 2452−2462.

(19) Coble, P. G.; Green, S. A.; Blough, N. V.; Gagosian, R. B. Characterization of dissolved organic matter in the Black Sea by fluorescence spectroscopy. *Nature* **1990**, *348*, 432−435.

(20) Guillemette, F.; del Giorgio, P. Simultaneous consumption and production of fluorescent dissolved organic matter by lake bacterioplankton. *Environ. Microbiol.* **2012**, *14* (6), 1432−1443.

(21) Yamashita, Y.; Tanoue, E. Chemical characterization of protein-like fluorophores in DOM in relation to aromatic amino acids. *Mar. Chem.* **2003**, *82* (3−4), 255−271.

(22) Hernes, P. J.; Bergamaschi, B. A.; Eckard, R. S.; Spencer, R. G. M. Fluorescence-based proxies for lignin in freshwater dissolved organic matter. *J. Geophys. Res.* **2009**, *114*, G00F03.

(23) Maie, N.; Scully, N. M.; Pisani, O.; Jaffe, R. Composition of a protein-like fluorophore of dissolved organic matter in coastal wetland and estuarine ecosystems. *Water Res.* **2007**, *41* (3), 563−70.

(24) Wagner, S.; Jaffe, R.; Cawley, K.; Dittmar, T.; Stubbins, A. Associations Between the Molecular and Optical Properties of Dissolved Organic Matter in the Florida Everglades, a Model Coastal Wetland System. *Front. Chem.* **2015**, *3*, 66.

(25) Amon, R. M. W.; Benner, R. Bacterial utilization of different size classes of dissolved organic matter. *Limnol. Oceanogr.* **1996**, *41* (1), 41−51.

(26) Kothawala, D. N.; Stedmon, C. A.; Muller, R. A.; Weyhenmeyer, G. A.; Kohler, S. J.; Tranvik, L. J. Controls of dissolved organic matter quality: evidence from a large-scale boreal lake survey. *Glob. Change Biol.* **2014**, *20* (4), 1101−14.

(27) McKnight, D. M.; Boyer, E. W.; Westerhoff, P. K.; Doran, P. T.; Kulbe, T.; Andersen, D. T. Spectrofluorometric characterization of dissolved organic matter for indication of precursor organic material and aromaticity. *Limnol. Oceanogr.* **2001**, *46* (1), 38−48.

(28) Aiken, G. R.; McKnight, D. M.; Thorn, K. A.; Thurman, E. M. Isolation of hydrophilic organic acids from water using nonionic macroporous resins. *Org. Geochem.* **1992**, *18* (4), 567−573.

(29) Aiken, G. R.; Thurman, E. M.; Malcolm, R. L. Comparison of XAD Macroporous Resins for the Concentration of Fulvic Acid from Aqueous Solution. *Anal. Chem.* **1979**, *51* (11), 1799−1803.

(30) Thurman, E. M.; Malcolm, R. L. Preparative Isolation of Aquatic Humic Substances. *Environ. Sci. Technol.* **1981**, *15* (4), 463−466.

(31) Serkiz, S. M.; Perdue, E. M. Isolation of Dissolved Organic-Matter from the Suwannee River Using Reverse-Osmosis. *Water Res.* **1990**, *24* (7), 911−916.

(32) Parlanti, E.; Worz, K.; Geoffroy, L.; Lamotte, M. Dissolved organic matter fluorescence spectroscopy as a tool to estimate biological activity in a coastal zone submitted to anthropogenic inputs. *Org. Geochem.* **2000**, *31* (12), 1765−1781.

(33) Ohno, T. Fluorescence inner-filtering correction for determining the humification index of dissolved organic matter. *Environ. Sci. Technol.* **2002**, *36* (4), 742−746.

(34) Zsolnay, A.; Baigar, E.; Jimenez, M.; Steinweg, B.; Saccomandi, F. Differentiating with fluorescence spectroscopy the sources of dissolved organic matter in soils subjected to drying. *Chemosphere* **1999**, *38* (1), 45−50.

(35) Murphy, K. R.; Stedmon, C. A.; Graeber, D.; Bro, R. Fluorescence spectroscopy and multi-way techniques. PARAFAC. *Anal. Methods* **2013**, *5* (23), 6557−6566.

(36) Murphy, K. R.; Stedmon, C. A.; Wenig, P.; Bro, R. OpenFluor- an online spectral library of auto-fluorescence by organic compounds in the environment. *Anal. Methods* **2014**, *6* (3), 658−661.

(37) Stenson, A.; Marshall, A.; Cooper, W. Exact masses and chemical formulas of individual Suwannee River fulvic acids from ultrahigh resolution electrospray ionization Fourier transform ion cyclotron resonance mass spectra. *Anal. Chem.* **2003**, *75* (6), 1275−1284.




DOI: 10.1021/acs.est.7b05513
*Environ. Sci. Technol.* 2018, 52, 2538−2548

(38) Koch, B.; Dittmar, T.; Witt, M.; Kattner, G. Fundamentals of molecular formula assignment to ultrahigh resolution mass data of natural organic matter. *Anal. Chem.* **2007**, *79* (4), 1758−1763.
(39) Corilo, Y. *EnviroOrg*. Florida State University, 2015.
(40) Koch, B. P.; Dittmar, T. From mass to structure: an aromaticity index for high-resolution mass data of natural organic matter. *Rapid Commun. Mass Spectrom.* **2006**, *20* (5), 926−932.
(41) Rossel, P. E.; Stubbins, A.; Hach, P. F.; Dittmar, T. Bioavailability and molecular composition of dissolved organic matter from a diffuse hydrothermal system. *Mar. Chem.* **2015**, *177*, 257−266.
(42) Raymond, P. A.; Bauer, J. E. Riverine export of aged terrestrial organic matter to the North Atlantic Ocean. *Nature* **2001**, *409*, 497−500.
(43) R Core Team, R. *A Language and Environment for Statistical Computing*; R Foundation for Statistical Computing: Vienna, Austria, 2015.
(44) Oksanen, J.; Blanchet, F. G.; Kindt, R.; Legender, P.; Minchin, P. R.; O'Hara, R. B.; Simpson, G. L.; Solymos, P.; Stevens, M. H. H.; Wagner, H. vegan: Community Ecology Package. *R package version 2.0−0*. http://CRAN.R-project.org/package=vegan.
(45) Harrell, F. E.; al., e. Hmisc: Harrell Miscellaneous. *R package version 3.17−2.*, 2016.
(46) Benjamini, Y.; Hochberg, Y. Controlling the False Discovery Rate - a Practical and Powerful Approach to Multiple Testing. *J. R. Stat. Soc. B* **1995**, *57* (1), 289−300.
(47) Poulin, B. A.; Ryan, J. N.; Aiken, G. R. Effects of Iron on Optical Properties of Dissolved Organic Matter. *Environ. Sci. Technol.* **2014**, *48* (17), 10098−10106.
(48) Spencer, R. G. M.; Butler, K. D.; Aiken, G. R., Dissolved organic carbon and chromophoric dissolved organic matter properties of rivers in the USA. *J. Geophys. Res.* **2012**, *117*, (G3).n/a10.1029/2011JG001928
(49) Jaffe, R.; Ding, Y.; Niggemann, J.; Vahatalo, A. V.; Stubbins, A.; Spencer, R. G. M.; Campbell, J.; Dittmar, T. Global Charcoal Mobilization from Soils via Dissolution and Riverine Transport to the Oceans. *Science* **2013**, *340* (6130), 345−347.
(50) DiDonato, N.; Chen, H.; Waggoner, D.; Hatcher, P. G. Potential origin and formation for molecular components of humic acids in soils. *Geochim. Cosmochim. Acta* **2016**, *178*, 210−222.
(51) Stubbins, A.; Niggemann, J.; Dittmar, T. Photo-lability of deep ocean dissolved black carbon. *Biogeosciences* **2012**, *9* (5), 1661−1670.
(52) Hertkorn, N.; Benner, R.; Frommberger, M.; Schmitt-Kopplin, P.; Witt, M.; Kaiser, K.; Kettrup, A.; Hedges, J. I. Characterization of a major refractory component of marine dissolved organic matter. *Geochim. Cosmochim. Acta* **2006**, *70* (12), 2990−3010.
(53) Mcknight, D. M.; Aiken, G. R.; Smith, R. L. Aquatic Fulvic-Acids in Microbially Based Ecosystems - Results from 2 Desert Lakes in Antarctica. *Limnol. Oceanogr.* **1991**, *36* (5), 998−1006.
(54) Azam, F. Microbial control of oceanic carbon flux: The plot thickens. *Science* **1998**, *280* (5364), 694−696.
(55) Horowitz, N. H.; Cameron, R. E.; Hubbard, J. S. Microbiology of the Dry Valleys of Antarctica. *Science* **1972**, *176*, 242−245.
(56) Hansell, D. A.; Carlson, C. A.; Repeta, D. J.; Schlitzer, R. Dissolved Organic Matter in the Ocean: A Controversy Stimulates New Insights. *Oceanography* **2009**, *22* (4), 202−211.
(57) Hedges, J. I.; Keil, R. G.; Benner, R. What happens to terrestrial organic matter in the ocean? *Org. Geochem.* **1997**, *27* (5/6), 195−212.
(58) Medeiros, P. M.; Seidel, M.; Niggemann, J.; Spencer, R. G. M.; Hernes, P. J.; Yager, P. L.; Miller, W. L.; Dittmar, T.; Hansell, D. A. A novel molecular approach for tracing terrigenous dissolved organic matter into the deep ocean. *Global Biogeochem. Cycles* **2016**, *30* (5), 689−699.


DOI: 10.1021/acs.est.7b05513
*Environ. Sci. Technol.* 2018, 52, 2538−2548